Meccanica
DOI 10.1007/s11012-014-9998-6

BRIEF NOTES AND DISCUSSIONS

Achieving uniform concentration by optimised dosage in a microchannel

Gianluca Mussetti · Jan O. Pralits · Andrea Mazzino

Received: 2 January 2014 / Accepted: 21 June 2014

1 Introduction

Mixing control in microchannels is a problem of paramount importance in a variety of situations ranging from applications in chemistry and biochemistry [1] to fundamental research in fluid mechanics and transport [2]. The main problem to solve is related to the fact that purely hydrodynamic fluid instabilities are inhibited due to negligible inertia of microchannel flow. Since mixing times or distances can be very long, strategies are required to enhance mixing in microdevices [3, 4]. Along this line, the suggestion of a new strategy is the main concern of our paper. Two different approaches are commonly used to induce mixing, according to their active or passive character [5]. Active micromixers use the disturbance generated by an external time-dependent field for the mixing process, eg., pressure gradient [6], electric fields [7] and sound [8]. Those methods are often difficult because of the tiny scales involved and they also pose several problems from a manufacturing point of view. Passive micromixer do not require external energy, the mixing process relies entirely on diffusion [9] or chaotic advection [4]. In the first approach, the molecular diffusion is enhanced by increasing the contact surface and decreasing the mixing path [9]. In the second, the geometrical structure of the microchannel is projected to trigger Lagrangian chaos (and thus mixing via eddy-diffusivity mechanisms [10–12]). Suitable non-Newtonian fluid solutions [17, 18] often provide an alternative valid answer to trigger mixing exploiting elastic instabilities in the limit of very small Reynolds numbers [13–16] or, eventually, turbulence [19–21].

Our aim here is to show how, exploiting state-of-the-art control/optimization techniques, the mixing of a passive scalar quantity emitted in a microchannel can be easily enhanced by a time-dependent injection in punctual and multi-source configuration. The control we propose relies on the optimal interplay between advection, injection and diffusion for the actual mixing. The technique is active but does not require any time-dependent variation of the emission source position. The system is especially suitable for noncontinuous mixing [22] and, at the same time, for dosing with a minimal emitted substance.

G. Mussetti (✉)
Dipartimento di Informatica, Bioingegneria, Robotica e Ingegneria dei Sistemi, Università di Genova, Via Montallegro 1, 16145 Genova, Italy
e-mail: mussetti.gianluca@gmail.com

G. Mussetti
CIMA Research Foundation, University Campus - via Magliotto 2, 17100 Savona, Italy

J. O. Pralits · A. Mazzino
Dipartimento di Ingegneria Civile, Chimica e Ambientale, Università di Genova, Via Montallegro 1, 16145 Genova, Italy

A. Mazzino
INFN and CINFAI Consortium, Via Dodecaneso 33, 16146 Genova, Italy

Published online: 04 July 2014

Table 1 Summary of the source configurations exploited in the analyzed cases

Case	Sources	Optimization
1 ref	F	OFF
1	F	ON
2	A,M	ON
4	A,B,L,M	ON
6	A,B,C,I,L,M	ON
8	all-(E,F,G)	ON
10	all-F	ON
11	all	ON

Refer to Fig. 1 for sources geometry and positions

2 Problem formulation

In this analysis we model the dispersion of a substance in a microchannel with infinite depth. A sketch of the domain is given in Fig. 1 where x and y denote the streamwise and cross stream directions, L the channel length and H the channel height, respectively. The governing equations are made dimensionless using the centerline velocity U_c^*, channel height H^*, diffusion coefficient κ^* and kinematic viscosity ν^*. Here, superscript $\{\}^*$ denotes dimensional quantity. The basic flow is considered laminar and given by the parabolic Poiseuille profile $u(y) = 1 - 4y^2$. The governing advection-diffusion equation in non-dimensional form is given as

$$\frac{\partial C}{\partial t} + u\frac{\partial C}{\partial x} - \frac{1}{Pe}\left(\frac{\partial^2 C}{\partial x^2} + \frac{\partial^2 C}{\partial y^2}\right) - S = 0, \tag{1}$$

where $C(x, y, t)$ is the concentration, $Pe = U_c^* H^*/\kappa^*$ the Péclet number and $S(x, y, t)$ a source term used to model the dosage. Moreover, the corresponding Reynolds and Schmidt numbers are defined as $Re = U_c^* H^*/\nu^*$ and $Sc = \frac{\nu^*}{\kappa^*}$ respectively. Note that S must be sufficiently small not to alter the (assigned) velocity profile. Equation (1) is accompanied with homogeneous conditions on the streamwise boundaries and no-flux conditions on the channel walls: $C(0, y, t) = 0$, $C(x_2, y, t) = 0$ and $\partial C(x, y, t)/\partial y|_{y=\pm 0.5} = 0$, and the initial condition is simply given by $C(x, y, 0) = 0$. The source term S represents a dosage source located at some fixed point (x_0, y_i) and modeled as $S(x, y, t) = s_i(t)\delta(x - x_0)\delta(y - y_i)$ where ith is the dosage concentration flux of the ith source and δ is the Dirac delta function.

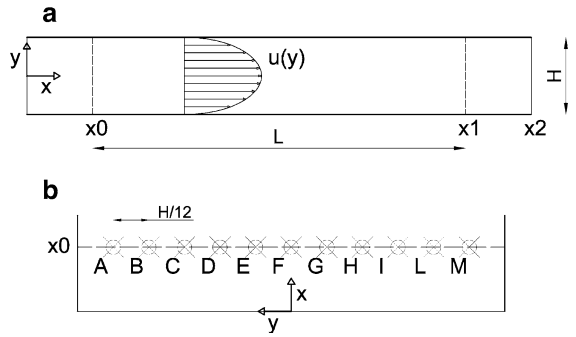

Fig. 1 **a** A sketch of the micropipe, where x_0, x_1 and x_3 are the inlet, target and outlet section, respectively. **b** A detailed view of the position of the sources

3 Optimal dosage

The aim is to compute an optimal dosage concentration $s_i(t)$ in a given time interval $0 \le t \le T$ which gives a desired concentration profile in the channel at a certain streamwise location, x_1, at the final time $t = T$. From a mathematical viewpoint, the optimization problem amounts to find the optimal $s_i(t)$ which minimizes the objective function

$$J = \int_0^L \int_{-0.5}^{0.5} h[C(x, y, T) - C_t]^2 \, dy \, dx, \tag{2}$$

where $h(x) = \exp[-(x - x_1)^6]$ is a bell-shaped function centered in $x = x_1$. The objective function quantifies the difference between the actual concentration C and the target C_t which we aim to obtain at a streamwise position $x = x_1$ at the final time $t = T$. The current constrained optimization problem can be recast on the unconstrained form by introducing the Lagrangian $\mathcal{L}$ as

$$\begin{aligned}\mathcal{L} = J &- \int_0^T \langle a, F(C, S)\rangle dt - \langle b_1(x, y), C(x, y, 0)\rangle \\ &- \int_0^T \int_{-0.5}^{0.5} [b_2(y, t)C(0, y, t) + b_3(y, t)C(L, y, t)] dy \, dt \\ &- \int_0^T \int_0^L \left[b_4 \frac{\partial C(x, -0.5, t)}{\partial y} + b_5 \frac{\partial C(x, 0.5, t)}{\partial y} \right] dx \, dt,\end{aligned} \tag{3}$$

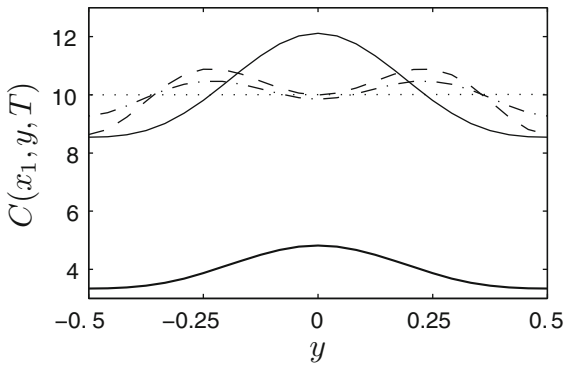

Fig. 2 Concentration profiles in the target section x_1 at time T, for $Pe = 150$, in the following cases: "1 ref" with the same total mass of the optimal case (*thick line*)," 1 ref" (*solid line*), "1" (*dashed*) and "11" (*dash-dot*). The *horizontal dotted line* indicates the target concentration value

where $F(C,S)$ denotes Eq. (1) and the inner product $\langle f,g\rangle = \int_0^L \int_{-0.5}^{0.5} f(x,y)g(x,y)\,dydx$ for two real-valued functions f and g. Here a and $b_{i=1..5}$ are the Lagrange multipliers and all variables are considered independent. The problem is solved by searching for a stationary point of Eq. (3). In practice this is made by setting the gradient of $\mathcal{L}$, with respect to each variable, to zero. In particular for the term $F(C,S)$ this is obtained by performing integration by parts in space and time in order to transfer the derivatives from C to a. The procedure is straight forward and the reader is referred to [23] for further details on the topic and to [24] for an application example. The gradients of $\mathcal{L}$ with respect to a and $b_{i=1,\ldots,5}$ give the governing Eq. (1) with boundary and initial conditions. The gradient of $\mathcal{L}$ with respect to C gives the adjoint equation and finally the gradient with respect to s gives the optimality condition. The adjoint equation is written

$$-\frac{\partial a}{\partial t} - u\frac{\partial a}{\partial x} - \frac{1}{Pe}\left(\frac{\partial^2 a}{\partial x^2} + \frac{\partial^2 a}{\partial y^2}\right) = 0, \tag{4}$$

with boundary conditions $a(0,y,t) = 0$, $a(\mathcal{L},y,t) = 0$ and $\partial a(x,y)/\partial y|_{y=\pm 0.5} = 0$, and initial condition $a(x,y,T) = 2h[C(x,y,T) - C_t]$. Note that the adjoint Eq. (4) is integrated backwards in time with the initial condition given at $t = T$. The gradient of the Lagrangian $\mathcal{L}$ with respect to the control term s_i is finally derived from Eq. (3) as

$$\frac{\partial \mathcal{L}}{\partial s_i} = -a(x_0, y_i, t) \tag{5}$$

The optimization problem is solved iteratively using the following scheme:

DO

1. Equation (1) is solved from $t = 0$ to $t = T$
2. Equation (4) is solved from $t = T$ to $t = 0$
3. Check $dJ = (J^{k+1} - J^k)/J^k$ *and* $\nabla_{s_i}\mathcal{L} = \frac{\partial \mathcal{L}}{\partial s_i}$
4. $k = k + 1$, $s_i^{k+1}(t) = s_i^k(t) - \rho(\frac{\partial \mathcal{L}}{\partial s_i})^k$

WHILE $dJ < \epsilon$ *and* $\nabla_{s_i}\mathcal{L} < \epsilon$

where $s_i(t)$ at the first iteration is given an arbitrary value and ϵ is a given real-valued convergence criteria.

4 Results and discussions

The results are obtained by numerically integrating the discretized equations (1) and (4), approximated using FTCS (Forward Time, Central Space) finite differences. The scheme is first-order explicit in time and second-order accurate in space. Numerical simulations are characterized by: $L = 5; H = 1; Pe = 100$ and 150; $T = 16; ds = 0.04; dt = 0.01; C_t = 10; \rho = 0.99$; $\epsilon = 0.005$. The corresponding Reynolds numbers are $Re = [\frac{100}{Sc}$ and $\frac{150}{Sc}]$. Several source configurations are tested, as summarized in Table 1 with reference to Fig. 1, in order to identify the benefits of a multi-source strategy. It is worth observing that, for uniaxial flows, the distance along the channel that is required for complete mixing to occur is $\Delta x_m \sim U_c \times (H^2/\kappa) = Pe\ H$ [4]. In this work, we compare the mixing results at a fixed distance $L = 5\ H$ using the above described optimization technique.

The results are compared against a reference case, here denoted by "1 ref", that achieves the same concentration mean value in the target section with a constant injection rate. The total mass injected is defined as

$$M = \int_0^T \sum_i s_i\ dt\ . \tag{6}$$

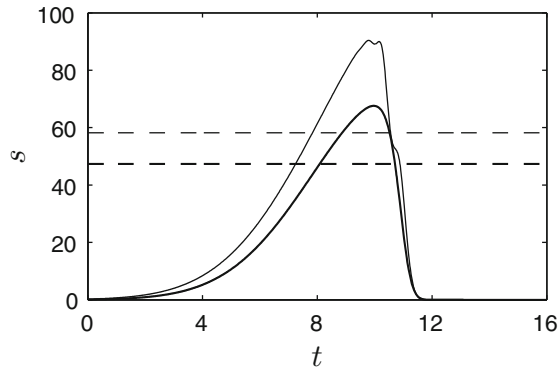

Fig. 3 Injection *curves* for the cases $Pe = 100$ (*thick line*) and $Pe = 150$ (*thin line*): "1 ref" (*dashed*), "1" (*solid*)

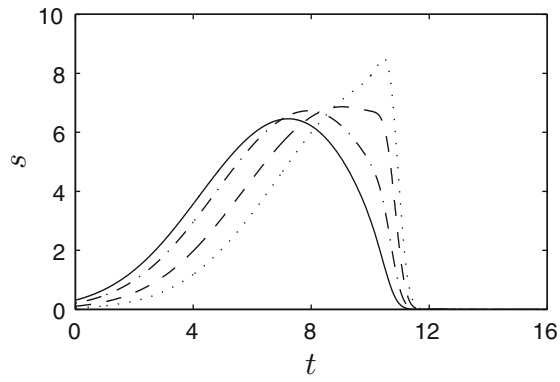

Fig. 4 Injection curves for the case "8", $Pe = 100$ for the source: A–M (*solid*), B–L (*dash-dot*), C–I (*dashed*) and D–H (*dotted*). Refer to Fig. 1 and Table 1 for details

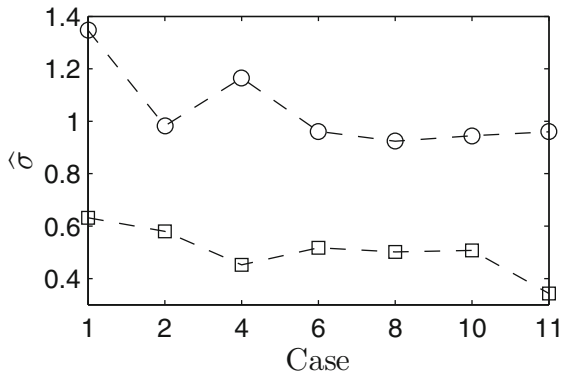

Fig. 5 Normalized standard deviation of the concentration $C(x, y, T)$ for all the cases indicated in Table 1. *Circle and square markers* indicate the cases $Pe = 100$ and $Pe = 150$, respectively

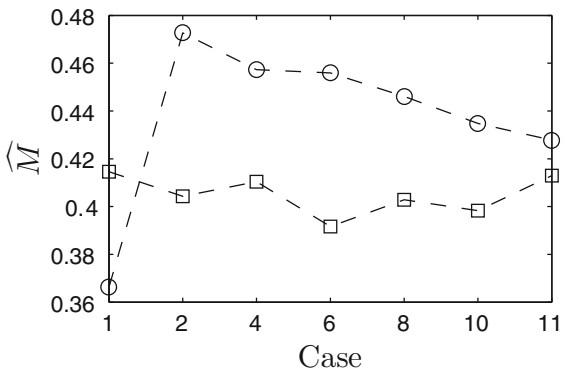

Fig. 6 Normalized total mass injected from 0 to T for all the cases indicated in Table 1. *Circle and square markers* indicate the cases $Pe = 100$ and $Pe = 150$, respectively

To quantify the degree of mixing, we measure the standard deviation of the concentration in the target section x_1, as

$$\sigma = \langle (C(x_1, y, T) - \langle C \rangle)^2 \rangle^{1/2} , \tag{7}$$

where $\langle\rangle$ means averages along the y direction. In order to compare model performances, σ and the total mass M are normalized using the reference case "1 ref", denoted by the subscript $_{ref}$, as $\hat{\sigma} = \frac{\sigma}{\sigma_{ref}}$ and $\hat{M} = \frac{M}{M_{ref}}$, respectively. Figure 2 shows the qualitative effects of the proposed mixing technique. The optimization system is able to avoid the central concentration lobe, typical of the dispersion in laminar flows. The multi-source configuration enhances the mixing, especially when the advective transport became predominant ($Pe = 150$). Figure 3 shows the shape of the optimal injection curves for the single source configuration. The substance is emitted with a discharge s that grows slightly until it reaches a peak at $t \approx T - T_A$, where $T_A = \frac{L}{U_C}$ is the so-called advective time. The first part of the injection curve is used to fill the boundary region of the target section. The robustness of the strategy is confirmed for a multi-source configuration, as represented in Fig. 4. The lateral sources (A–M,B–L and C–I) provide the substance for the boundary region, characterized by a low advective transport, while the internal sources (D–H) supply the core region at about the advective time T_A. Figure 5 represents the mixing performances for the various cases with respect to the reference case. The mixing enhancement is more effective for $Pe =$

150 than $Pe = 100$. As expected, the best results are associated with the maximum number of sources ($n = 11$). Besides, some intermediate cases offer interesting trade-offs, such as $n = 2$ and $n = 4$ for $Pe = 100$ and $Pe = 150$, respectively. Moreover, the proposed technique allows to strongly reduce the emitted quantity with respect to the reference case, as indicated in the Fig. 6. In general, the injected mass is more than halved and the effect increases using a multi-source configuration.

Acknowledgments A.M. and J.O.P. thank the financial support from the PRIN 2012 project n. D38C13000610001 funded by the Italian Ministry of Education. A.M. thanks the financial support for the computational infrastructure from the RITMARE project.

References

1. Whitesides GM (2006) The origin and the future of microfluidics. Nature 44:368–373
2. Tabeling J (2005) Introduction to microfluidics. Oxford University Press, New York
3. Squires TM, Quake SR (2005) Microfluidics: fluid physics at the nanoliter scale. Rev Mod Phys 77:977–1026
4. Stroock AD, Dertinger SKW, Ajdari A, Mezic I, Stone HA, Whitesides GM (2002) Chaotic mixer for microchannels. Science 295:647–651
5. Nguyen NT, Wu Z (2005) Micormixers—a review. J Micromech Microeng 15:R1R16
6. Deshmukh AA, Liepmann D, Pisano AP (2000) Continous micromixer with pulsatile micropumps. Tecnical Digest of the IEEE Solid State Sensor and Actuator Workshop, pp 73–76
7. Ajdari A (1995) Electro-osmosis on inhomogeneously charged surfaces. Phys Rev Lett 75:755–758
8. Yang Z (2001) Ultrasonic micromixer for microfluidic system. Sensor Actuators A 93:266–272
9. Miyake R, Lammerink TSJ, Elwenspoek M, Fluitman JHJ (1993) Proceedings of MEMS'97, 10th IEEE international workshop micro electromechanical system, pp 248–253
10. Biferale L, Crisanti A, Vergassola M, Vulpiani A (1995) Eddy diffusivities in scalar transport. Phys Fluids 7:2725–2734
11. Mazzino A (1997) Effective correlation times in turbulent scalar transport. Phys Rev E 56:5500–5510
12. Mazzino A, Musacchio S, Vulpiani A (2005) Multiple-scale analysis and renormalization for preasymptotic scalar transport. Phys Rev E 71:011113
13. Larson RG, Shaqfeh ESG, Muller SJ (1990) A purely viscoelastic instability in Taylor–Couette flow. J Fluid Mech 218:573–600
14. Boffetta G, Celani A, Mazzino A, Puliafito A, Vergassola M (2005) The viscoelastic Kolmogorov flow: eddy viscosity and linear stability. J Fluid Mech 523:161–170
15. Boffetta G, Celani A, Mazzino A, Puliafito A, Vergassola M (2007) Nonlinear dynamics of the viscoelastic Kolmogorov flow. J Fluid Mech 590:61–90
16. Boi S, Mazzino A, Pralits JO (2013) A minimal model for zero-inertia instabilities in shear-dominated non-Newtonian flows. Phys Rev E 88:033007
17. Ashmawy EA (2012) Unsteady Couette flow of a micropolar fluid with slip. Meccanica 47:85–94
18. Postelnicu A (2012) Free convection from a truncated cone subject to constant wall heat flux in a micropolar fluid. Meccanica 47:1349–1357
19. Groisman A, Steinberg V (2000) Elastic turbulence in a polymer solution flow. Nature 405:53–55
20. Berti S, Bistagnino A, Boffetta G, Celani A, Musacchio S (2008) Two-dimensional elastic turbulence. Phys Rev E 77:055306R
21. Boffetta G, Celani A, Mazzino A (2005) Drag reduction in the turbulent Kolmogorov flow. Phys Rev E 71:036307
22. Voldman J, Gray ML, Schmidt MA (2000) An integrated liquid mixer/valve. Microelectromech Syst 9:295–302
23. Gilbert JC, Lemarechal C (2006) Numerical optimization: theoretical and practical aspects. Springer, Berlin
24. Pralits JO, Hanifi A, Henningson DS (2002) Adjoint-based optimization of steady suction for disturbance control in incompressible flows. J Fluid Mech 467:129–161